

Zinc Oxide Nanorods as H₂S Gas Sensor

Yogita S. Patil¹, F. C. Raghuvanshi², I. D. Patil³

¹ Department of Applied Science, Government College of Engineering, Jalgaon

² Principal, Vidya Bharati Mahavidyalaya, Amravati

³ Department of Biotechnology, SSBT's College of Engineering, Jalgaon

Abstract: *The zinc oxide nanorods have been synthesized and studied as the sensing element for the detection of H₂S gas. The zinc oxide nanorods were synthesized by precipitation method. The thick films of synthesized material were prepared by screen printing method on glass substrate. Gas sensing properties of zinc oxide thick films were studied for H₂S, LPG and NH₃ gases by changing the concentration of test gases. The prepared zinc oxide thick films can be used as promising material for semiconductor gas sensor for poisonous gases like H₂S with high sensitivity.*

Keywords: zinc oxide nanorods, thick film, H₂S gas sensor

1. Introduction

Hydrogen sulphide (H₂S) is a toxic and inflammable gas, produced in sewage plants, coal mines and oil and natural gas industries. It is used in large amounts in various chemical industries, research laboratories and as a process gas in the production of heavy water. Although the occupational exposure limit for the gas is 10 ppm for 8 h exposure, the acceptable ambient levels of H₂S (recommended by the Scientific Advisory Board on Toxic Air Pollutants, USA) are in the range of 20–100 ppb [1]. Therefore, it is required to detect H₂S at these low levels. Spectral and fluorescence analysis [2,3] may be used for detecting low concentrations of this gas but these sensors have high cost and large size. Semiconductor gas sensors have proved to be a low cost and convenient option for monitoring of gas species and sensors in the form of thin or thick films, based on metal oxides like SnO₂, WO₃ and p–n heterojunctions (SnO₂–CuO), have been reported for detection of H₂S gas [4–8] in a ppm range. Recently such sensors for low concentrations have also been reported [9–12].

Zinc oxide (ZnO), with a wide band gap (3.4 eV) and a large excitation binding energy (60 meV), has attracted remarkable attention for its electronic and photonic applications such as ultraviolet (UV)/blue light-emitting devices, solar is used in Solar cells, piezoelectric devices, acousto-optical devices and chemical sensors [13] and [14]. Nowadays, the development of gas sensors to detect volatile and toxic gases is imperative due to the concerns for environmental pollution and the safety requirements of industry and daily life. ZnO has been considered as a promising material of gas sensors because of its high electrochemical stability, non-toxicity, suitability to doping, and low cost [15].

The sensing characters of a sensor depend on the shape and dimensionality of the sensing material a lot, so that multiplicate ZnO nanostructures have been synthesized and studied in the past decade. Researches have shown that one-dimensional (1D) ZnO nanostructures possess a large surface-to-volume ratio, which can absorb more tested molecules on the

surface [16], [17], [18], [19], [20], [21] and [22]. Up to now, 1D ZnO nanostructures, such as nanotubes, nanowires, nanorods and nano-tetrapods [15], [16], [17], [18], [19], [20], [21] and [22], have been synthesized by various physical and chemical methods and used to fabricate gas sensors.

In this work, we develop a simple precipitation method to synthesize the bundle of rod-like ZnO nanostructure in high yield, starting with zinc nitrate hexa hydrate in aqueous solution as a precursor, and sodium hydroxide as a reducing agent. The ZnO nanorods were employed to construct a gas sensor by screen printing method for detecting H₂S gas.

2. Experimental

A. Preparation of Nanocrystalline ZnO Powder

In preparation of ZnO nanorods, 0.45 M aqueous solution of zinc nitrate (Zn(NO₃)₂·6H₂O) and 0.9 M aqueous solution of sodium hydroxide (NaOH) were prepared in distilled water. Then the beaker containing NaOH solution was heated at the temperature of about 55^oC. The zinc nitrate solution was added dropwise to the above heated solution. The precipitation was started to obtain when about 7 mL of zinc nitrate solution was added to the heated NaOH solution. The complete zinc nitrate solution was added to NAOH solution in about 45 minutes. The beaker was sealed at this condition for 1 hour. Then the precipitate was washed 2-3 times with the deionised water and absolute ethanol. The precipitate was dried at 70^oC in oven.

B. Gas-Sensing System to Check Gas-Sensing Performance



Figure 2: Static Gas sensing system

Figure 2 represents the photograph of the system for testing the sensing performance of the nanocrystalline ZnO thick-film sensors. There are electrical feeds through the base plate. The heater is fixed on the base plate. A sample under test can be mounted on the heater. The Cr–Al thermocouple is mounted to measure the operating temperature. The output of the thermocouple is connected to a temperature indicator. A gas inlet valve is fitted at one of the ports of the base plate. The gas concentration inside the static system is achieved by injecting a known volume of a test gas with a gas-injecting syringe. Constant voltage is applied to the sensor and the current is measured by a current meter.

C. Preparation of thick films

The thixotropic paste was screen printed on glass substrate in desired patterns. Fluidity of the paste depends up on extent of organic part, which goes in its formulation i.e on solid to liquid ratio. Paste must exhibit a certain degree of yield such that after flow occurs under squeegee pressure, it should stiffen and remain in position to have sharp line defined patterns to be printed that should have thixotropic properties.

In present process, thixotropic paste was formulated by mixing the synthesized ZnO powder with ethyl cellulose a temporary binder in a mixture of organic solvents such as butyl cellulose, butyl carbitol acetate and turpeneol. The ratio of ZnO to ethyl cellulose was kept at 95:05. The ratio of inorganic to organic part was kept as 75:25 in formulating the pastes. The thixotropic pastes were screen printed on a glass substrate in desired patterns. The prepared thick films were dried under IR lamp. The films prepared were fired at 550°C.

D. Characterizations

The X-ray diffraction (XRD) patterns of the obtained samples were recorded by D8Advance, Bruker, Germany. FESEM with EDAX images were taken on Hitachi Hitechnologies corporation, Japan (Model No. S4800). The UV-visible spectra of the sample was recorded.

3. Results

A. Characterizations of as Prepared Nanopowder

1) Structural Analysis:

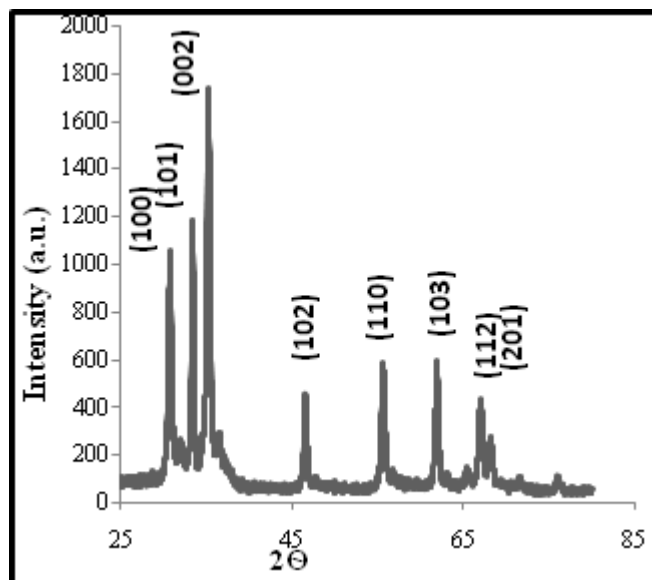


Figure 3: X-ray diffractogram of as prepared ZnO nanopowder.

Figure 3 shows the X-ray diffractogram of the as prepared ZnO nanopowder. Sharp intense peaks are obtained for ZnO corresponding to the planes (100), (101), (002), (102), (110), (103), (112), (201) these are associated with the hexagonal wurtzite structure of ZnO. It seems that these ZnO particles possess high crystallinity, since the peaks are very sharp.

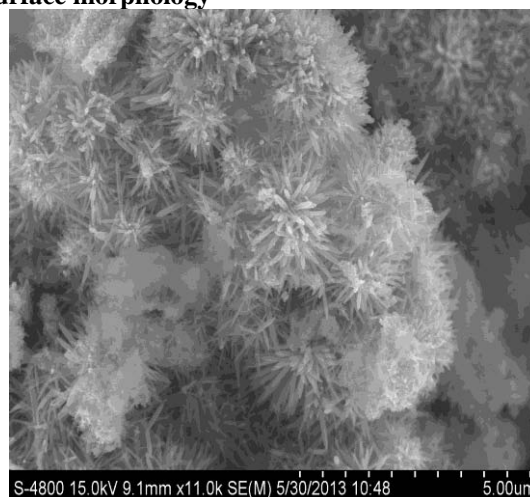
2. Crystallite size

The crystallite size is calculated from Debye Scherrer's formula

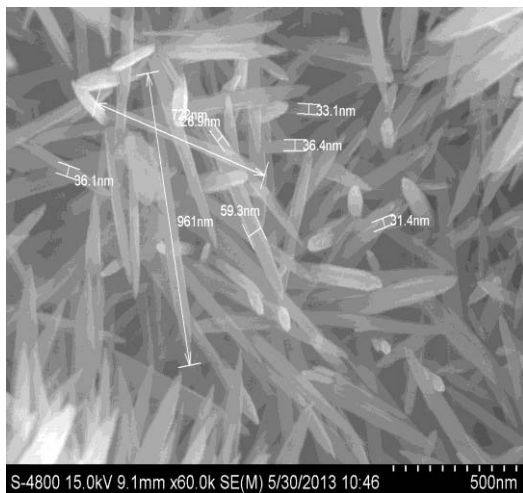
$$D = 0.9\lambda / B \cos \Theta$$

Where λ is the wavelength of radiation, B is full-width- at half- maxima in radians and Θ is characteristic X-ray radiation. The average crystallite size is found to be 25 nm for ZnO.

3. Surface morphology



(a)



(b)
Figure 4: FESEM images of ZnO nanorods

Figure 4 (a) and (b) shows FESEM images of ZnO nanorods. The image (a) shows a bulk quantity of flower like bunches for 30K resolution. Each bunch is formed due to gathering of closely packed nanorods while for 60K resolution the crystal structure is rod like. The nanorods are randomly distributed in the powdered sample. The diameter of rod ranges from 30nm to 60nm and the maximum length of the rod is found to be 961 nm. The images show high aspect ratio.

4) EDAX for Elemental Analysis

Figure 5 shows EDAX for elemental analysis of ZnO nanorods. Theoretically expected mass percentage of Zn and O in stoichiometric ZnO are expected to be 80.3 and 19.7, respectively. The observed values of mass percentage of Zn and O are represented in Table III.

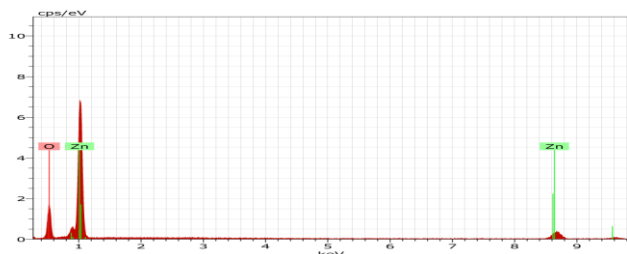


Figure 5: EDAX of ZnO using zinc nitrate as precursor

Table 3: EDAX for Elemental Analysis

El	AN	Series	unm. [wt.%]	C norm. [wt.%]	C Atom. [at.%]	CError (1 Sigma) [wt.%]
O	8	K-series	17.97	28.16	61.57	2.69
Zn	30	K-series	45.84	71.84	38.43	1.76
Total:			63.80	100.00	100.00	

5) Optical Absorption

UV-visible spectroscopy was carried out to study the optical property of the nanorods. The room temperature UV-absorption spectra of the ZnO nanorods are shown in figure 6. The sharp of the absorption edge suggests a single phase. The band-gap energy calculated from the absorption spectra is 3.37 eV, matches exactly with reported band gap energy (3.37 eV) of ZnO. It is interesting to note that the

nanocrystalline nature does not have a significant effect on the band gap of the nanocrystalline ZnO powder.

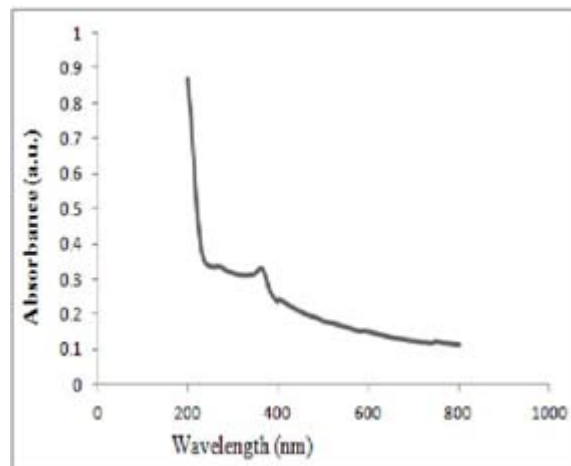


Figure 6: UV vis Absorption Spectrum of ZnO nanorods

5) Thickness Measurement of ZnO thick films

The thickness of ZnO thick films was measured by using Marutek film thickness measurement system. Thickness of films was observed in the range from 25µm to 35µm.

6) Electrical Measurement of thick films

The Current- Voltage Characteristics of ZnO thick film at different temperatures was measured.

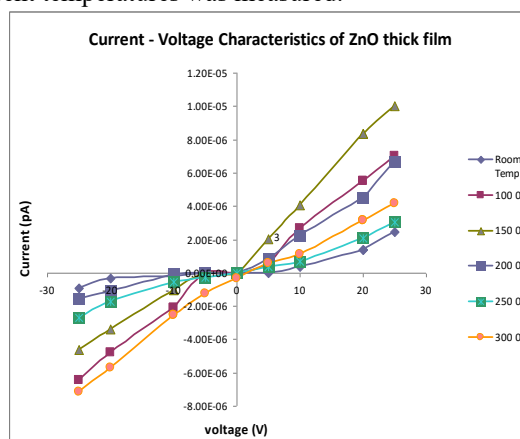


Figure 7: Current Voltage characteristics of ZnO thick films

Fig. 7 shows the Current Voltage characteristics of ZnO thick film at room temperature, 100 °C, 150 °C, 200 °C, 250 °C, 300 °C and that are observed symmetrical in nature. Current was measured while the bias voltage increased from 0 to 25 volts with the step of 5 volt. The measurement was repeated with negative voltage. The symmetrical nature of the I-V characteristics for the sample shows the contacts are ohmic in nature.

7) Electrical Conductivity

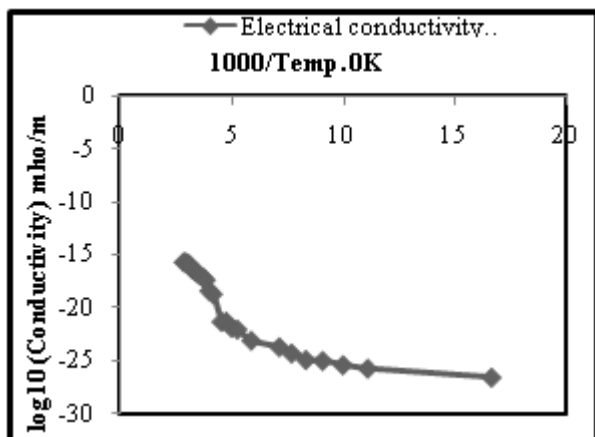


Figure 8: Conductivity temperature profile of ZnO thick film

Figure 8 shows the variation of log (conductivity) with temperature. The conductivity values of ZnO thick film increases with increase in operating temperature. They are nearly linear to $1/T$ in the range from 100°C to 250°C . The increase in conductivity with increasing temperature could be attributed to the negative temperature coefficient of resistance and semiconducting nature of the ZnO films. The conductivity increases exponentially during 250°C to 350°C and suddenly increases beyond 350°C . It is observed from Fig. 4.8.2 that the electrical conductivity of the ZnO film is larger.

8) Gas sensing performance of thick film:

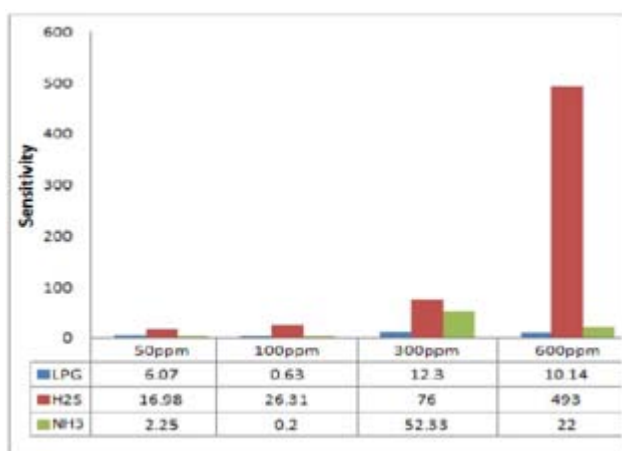


Figure 9: Gas response of ZnO thick film.

Figure 9 shows the gas responses of ZnO thick film for 100ppm, 300ppm and 600 ppm gas concentration at 200°C temperature to LPG, H_2S , and NH_3 gases. ZnO thick film sensor shows response to H_2S gas at 200°C . The higher response of ZnO thick film upon exposure to H_2S may be attributed to decrease in the concentration of oxygen adsorbents ($\text{O}^{2-}_{\text{ad}}$) and resulting increase in concentration of electron.

4. Conclusions

In this study, the structural, morphological, optical and gas sensing properties of ZnO nanorods have been studied. The ZnO nanorods are synthesized by simple chemical precipitation method. The structural characterization of the

nanorods showed hexagonal wurtzite structure. The flower like bunches are obtained for 30k resolution while for 60k resolution, crystal structure is rod like in FESEM results. The diameter of the rod ranges from 20 nm to 93 nm and the maximum length of the rod was found to be 961 nm. The band-gap of ZnO synthesized by using zinc nitrate as precursor and sodium hydroxide as reducing agent was calculated from an absorption spectrum and is found to be 3.37 eV. This value matches exactly with the reported value. The thick films were prepared by screen printing method and thickness of films was observed in the range from $25\mu\text{m}$ to $35\mu\text{m}$. The response of the nanocrystalline ZnO-based sensor was observed to be the largest to H_2S gas.

References

- [1] <http://daq.state.nc.us/toxics/studies/H2S/>
- [2] J. Chou, Hazardous Gas Monitors—A Practical Guide to Selection, Operation and Application, SciTech Publishing, 2000.
- [3] R.K. Stevens, J.D. Mulik, A.E. O’Keeffe, K.J. Krost, Gas chromatography of reactive sulfur gases in air at the parts-per-billion level, Anal. Chem. 43 (1971) 827–831.
- [4] A. Khanna, R. Kumar, S.S. Bhatti, CuO-doped SnO₂ thin films as hydrogen sulfide gas sensor, Appl. Phys. Lett. 82 (2003) 4388–4390.
- [5] V.R. Katti, A.K. Debnath, K.P. Muthe, M. Kaur, A.K. Dua, S.C. Gadkari, S.K. Gupta, V.C. Sahni, Mechanism of drifts in H₂S sensing properties of SnO₂:CuO composite thin film sensors prepared by thermal evaporation, Sens. Actuators B 96 (2003) 245–252.
- [6] J. Watson, The tin oxide gas sensor and its applications, Sens. Actuators 5 (1984) 29–42.
- [7] E.P.S. Barrett, G.C. Georgiades, P.A. Sermon, The mechanism of operation of WO₃-based H₂S sensors, Sens. Actuators B 1 (1990) 116–120.
- [8] A. Chowdhuri, P. Sharma, V. Gupta, K. Sreenivas, K.V. Rao, H₂S gas sensing mechanism of SnO₂ films with ultrathin CuO dotted islands, J. Appl. Phys. 92 (2002) 2172–2180.
- [9] R. Ionescu, A. Hoel, C.G. Granqvist, E. Llobet, P. Heszler, Low-level detection of ethanol and H₂S with temperature-modulated WO₃ nanoparticle gas sensors, Sens. Actuators B 104 (2005) 132–139.
- [10] B. Esfandyarpour, S. Mohajezadeh, A.A. Khodadadi, M.D. Robertson, Ultrahighsensitive tin-oxide microsensors for H₂S detection, IEEE Sens. J. 4 (2004) 449–454.
- [11] C.H. Wang, X.F. Chu, M.M. Wu, Detection of H₂S down to ppb levels at room temperature using sensors based on ZnO nanorods, Sens. Actuators B 113 (2006) 320–323.
- [12] M. Kaur, S. Bhattacharya, M. Roy, S.K. Deshpande, P. Sharma, S.K. Gupta, J.V. Yakhmi, Growth of nanostructures of Zn/ZnO by thermal evaporation and their application for room temperature sensing of H₂S gas, Appl. Phys. A 87 (2007) 91–96.
- [13] M.H. Huang, S. Mao, H. Feick, J.Q. Yan, Y.Y. Wu, H. Kind, E. Weber, R. Russo, P.D. Yang Room-temperature ultraviolet nanowire nanolasers Science, 292 (2001), pp. 1897–1899
- [14] O.D. Jayakumar, N. Manoj, V. Sudarsan, C.G.S. Pillai, A.K. Tyagi A rare defect free 3D ZnO rod structure

- with strong UV emission CrystEngComm, 13 (2011), pp. 2187–2190
- [15] J.X. Wang, X.W. Sun, Y. Yang, C.M.L. Wu N–P transition sensing behaviors of ZnO nanotubes exposed to NO₂ gas Nanotechnology, 20 (2009), p. 465501 (4pp)
- [16] D. Zhang, S. Chava, C. Berven, S.K. Lee, R. Devitt, V. Katkanant Experimental study of electrical properties of ZnO nanowire random networks for gas sensing and electronic devices Appl. Phys. A, 100 (2010), pp. 145–150
- [17] C.M. Chang, M.H. Hon, I.C. Leu Preparation of ZnO nanorod arrays with tailored defect-related characteristics and their effect on the ethanol gas sensing performance Sens. Actuators B, 151 (2010), pp. 15–20
- [18] J.Q. Xu, Y.P. Chen, D.Y. Chen, J.N. Shen Hydrothermal synthesis and gas sensing characters of ZnO nanorods Sens. Actuators B, 113 (2006), pp. 526–531
- [19] L. Li, H.Q. Yang, H. Zhao, J. Yu, J.H. Ma, L.J. An, X.W. Wang Hydrothermal synthesis and gas sensing properties of single-crystalline ultralong ZnO nanowires Appl. Phys. A, 98 (2010), pp. 635–641
- [20] J. Kim, K. Yong Mechanism study of ZnO nanorod-bundle sensors for H₂S gas sensing J. Phys. Chem. C, 115 (2011), pp. 7218–7224
- [21] Y.Y. Zhang, J. MuControllable synthesis of flower- and rod-like ZnO nanostructures by simply tuning the ratio of sodium hydroxide to zinc acetate Nanotechnology, 18 (2007), p. 075606 (6pp)
- [22] X.F. Chu, D.L. Jiang, B.D. Aleksandra, H.L. Yu Gas-sensing properties of thick film based on ZnO nanotetrapods Chem. Phys. Lett., 401 (2005), pp. 426–429